Design and development of novel layered nanostructured hybrid materials for environmental, medical, energy and catalytic applications

Potsi, Georgia

CHAPTER 4

Oxidized carbon nanodiscs as cytotoxic agents

In this work we report the fabrication of soluble hydrophilic carbon nanodiscs by the chemical oxidation of insoluble pristine carbon nanodiscs (CNDs) using the method that is commonly used for the graphite oxidation. The pristine CNDs were prepared through the pyrolytic Kvaerner Carbon Black & H_2 process using an industrial-scale carbon-arc plasma torch generator. The oxidized product is decorated with various oxygen-containing functional polar groups, converting the insoluble CNDs to a hydrophilic derivative that can be easily disperse in polar solvents including water. These hydrophilic derivatives are expected to find application a wide range of fields including biomedicine. In this work they were tested as antiproliferative agents for two cell lines, a healthy and a cancer one, in order to investigate their cytotoxic properties.

This Chapter is partially based on the article by P. Zygouri, T.Tsoufis, A. Kouloumpis, M. Patila, G.Potsi, Z. Sideratou, F. Katsaros, G. Charalambopoulou, H. Stamatis, P. Rudolf, T. A. Steriotis and D. Gournis, Hydrophilic oxidized carbon nanodiscs: A promising multifunctional nanocarbon for bioapplications, to be submitted.

4.1. Introduction

Among the many nanomaterials synthesized the last decades carbon nanostructured materials occupy the most prominent position. This is due to the unusual potential of carbon to form many allotropes thanks to its sp^3, sp^2 and sp hybridization. Carbon low-dimensional nanostructures include the 0D fullerenes, the 1D carbon nanotubes and the 2D graphene. Their discovery and investigation[1][2]lead to two Nobel prizes awarded to Kroto, Smalley, Curl in 1996 for the discovery of fullerenes and to Novoselov and Geim in 2010 for the discovery of graphene. Carbon nanostructures distinguish themselves for low density, high specific surface, tunable pore structure, chemical stability as well as the excellent electronic, thermal and mechanical properties and hence are promising candidates for a wide range of applications including organic electronic[3]photovoltaics,[4]biological and medical applications,[5][6] catalyst supports,[7] field emission devices,[8] nanoprobes,[9] sensors,[8] semiconductor devices,[10] composite materials (polymeric or ceramic),[11][12][13][14] nanoelectronics,[15] gas separations,[7] supercapacitors,[16] and energy storage materials[17].

Carbon nanodiscs (CNDs), are synthesized through the so-called pyrolytic Kvaerner Carbon Black & H_2 (CB&H) Process, [18][19] where hydrocarbons (typically heavy oil) are decomposed to carbon and H_2 based on the use of an industrial-scale carbon-arc plasma torch generator operating at a temperature around 2000 ^{o}C. The carbon product consists of three different turbostratic graphitic microstructures, namely flat CNDs (no pentagons), conical carbon structures (1-5 pentagons) and amorphous carbon (soot), with volume fractions around 82 %, 5 % and 13 %, respectively[19]. CNDs are micron sized, ultrathin quasi two-dimensional particles with diameter 1-4 μm, while the co-existing carbon cones are of similar size. Garberg *et al*.[20] showed that CNDs are multilayer structures with a graphitic core and outer non-crystalline layers. CNDs are considered to have homogeneous thickness, typically in the range 10–30 nm. The degree of graphitization can be greatly promoted by post heat-treatment at 2700 ^{o}C under argon[21]. Annealed CNDs and cones are almost single

crystalline in the c-direction and may thus be considered as stacks of a limited number of graphene layers (usually < 100)[21].

The size of these disc-like carbon nanostructures is large enough to maintain important graphite properties such as electrical conductivity and on the other hand, small enough and even ideal in some cases, for applications in biotechnology, nanomedicine and drug delivery. The main disadvantage of CNDs is that - like all other carbon structures - they are insoluble in polar solvents, which renders them difficult to process.

Chemical modification of their surface is a solution to this problem since it improves their ability to disperse in organic solvents and water. It is thus through functionalization that they become more compatible with other materials and more easily included in the preparation of composites. The aim of this project is to apply a simple and reproducible approach for the chemical oxidation of CNDs, similar to the well-known Staudenmaier's method[22]that has been applied for the chemical oxidation of graphite[23][24]. As we shall show in the following, strong acid treatment results the CND surface decoration with various oxygen-containing functional polar groups such as hydroxyl, carboxyl and epoxy groups. These functional groups convert the CNDs into a hydrophilic derivative, which is completely soluble in polar solvents including water. A beneficial side effect of the acid treatment is that it also separates the CNDs from the nanocones and soot in the mixed starting material. A number of characterization techniques was applied to characterize the functionalized nanodiscs, namely Fourier transform infrared (FTIR), μ-Raman and X-ray photoelectron spectroscopies, X-ray diffraction, thermogravimetric analysis (DTA/TGA) and atomic force microscopy (AFM). Oxidized carbon nanodiscs are expected to have a wide range of diverse applications in the chemical and pharmaceutical industry, as well as in electronics. In this project we tested the cytotoxic properties of oxCNDs on two different cell lines in order to investigate potential future applications in biomedicine and bio-catalysis.

4.2. Results and discussion

To verify that the oxidation of CNDs results in the creation of oxygen containing groups covalently attached on the surface of the discs similarly to graphene oxide, we employed FTIR and XPS spectroscopies. The FTIR spectra of pristine and oxidized carbon nanodiscs are shown in Figure 4.1. Contrary to the pristine CNDs oxidized carbon nanodiscs exhibit intensive vibrational bands in the region of 1000-1700 cm^{-1}. More specifically, the band at 1058 cm^{-1} is assigned to stretching vibrations of C–O groups, while the weak peak at 1405 cm^{-1} is due to bending vibrations (deformation) of hydroxyl groups C-OH groups [25][26]. The band at 1620 cm^{-1} is attributed to the C=O stretching vibrations of the –COOH groups[26], while the the band at 1230cm^{-1} is assigned to asymmetric stretching of C-O-C bridges in epoxy groups and to deformation vibrations of O-H in the carboxylic acid groups. The presence of all these characteristic vibrational bands testifies to the successful oxidation of the carbon nanodiscs.

The XPS spectrum of the C1s core level region of oxCNDs shown in Figure 4.2 can be deconvoluted in three main contributions: the first peak at a binding energy of 284.8 eV is assigned to the C-C bonds of the graphitic framework[27] and accounts for 82.4 %

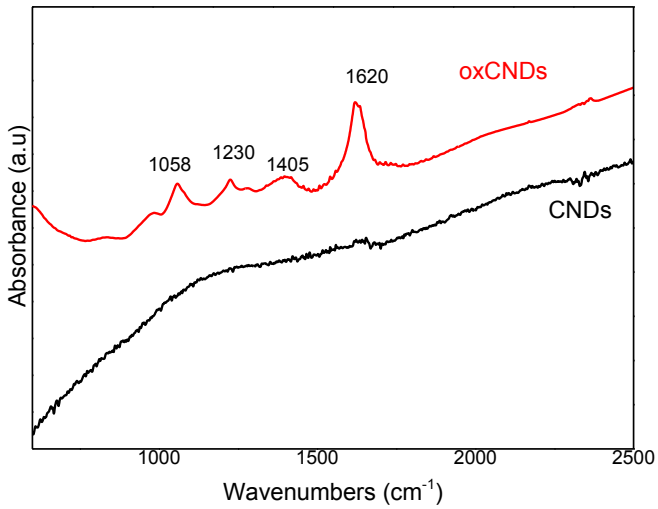

Figure 4.1. FT-IR spectra of pristine (black) and oxidized carbon nanodiscs (red).

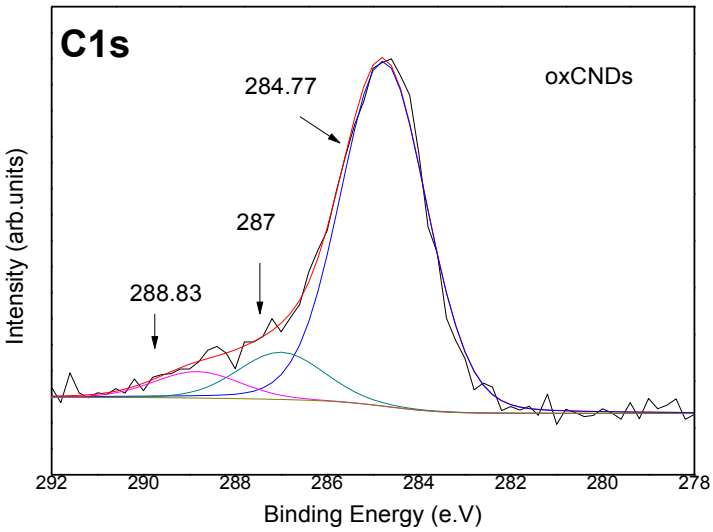

Figure 4.2. XPS spectrum of the C 1s core level region of oxidized carbon nanodiscs (oxCNDs).

of the overall carbon 1s intensity; a second peak attributed to C-O bonds at 287.0 eV makes up 11.2 % of the total C1s intensity, while a third contribution at 288.8 e.V (6.2% of the overall C1s intensity) is assigned to O-C=O bonds.[28][29] These contributions from C-O, C=O and O-C=O bonds do not appear in the corresponding XPS spectrum of the starting material[30] and hence the oxygen-containing groups must have formed during the strong acidic treatment of the CNDs. The oxidation process is therefore similar to that of graphene oxide produced from graphite with the Staudenmaier's method.[29][31][32][33][34]

An additional technique that confirmed the successful oxidation of CNDs was Raman spectroscopy. The Raman spectra of pristine and oxidized carbon nanodiscs are presented in **Figure 4.3.** Both show the characteristic first-ordered G- and D- bands at around 1600 and 1350 cm^{-1}, respectively. The G-band originates from the doubly degenerate *E*2*g* mode around the Brillouin zone centre and is associated with sp^2-hybridized carbon atoms. The D-band is related to sp^3 hybridized carbon atoms as it

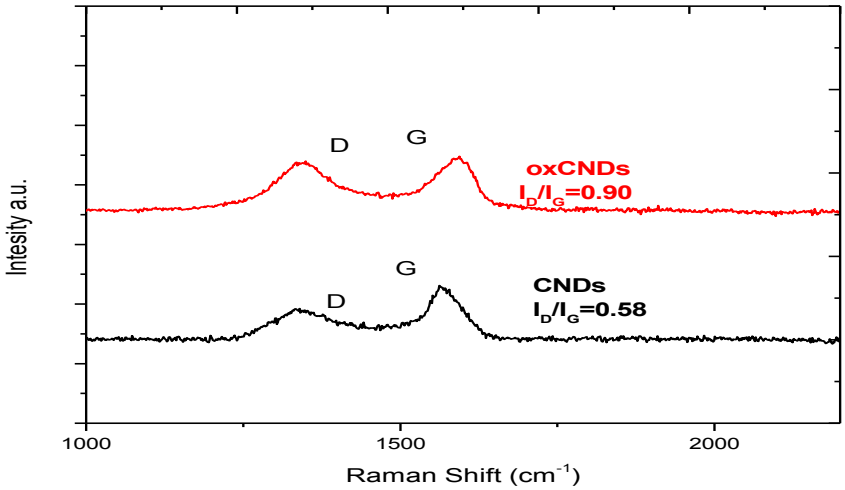

Figure 4.3. Raman spectra of pristine CNDs (black) and oxCNDs (red)

requires a defect or an edge for its activation by double resonance, thus indicating the presence of lattice defects and distortions.[35][36][37][38]The ratio of the D- to G-band intensities (I_D/I_G) is indicative of the quality of the graphitic lattice and was found to be 0.57 for the pristine CNDs. The important increase of the I_D/I_G ratio in oxCND sheets which is at least 0.90 as can be postulated via the relative increase of the D' band (1620 cm^{-1}) which exceeds the intensity of the G band[39] confirms the change in the hybridization of the carbon atoms from sp^2 to sp^3, due to the creation of oxygenated groups (hydroxyl, carboxyl or epoxide) that are covalently attached to the double bonds of aromatic groups.

The results from the thermogravimetric analysis (TGA) of pristine and oxidized carbon nanodiscs are shown in Figure 4.4. In the pristine CNDs, the major drop in the mass is observed around 630 ^oC, followed by complete decomposition of the material, indicating the thermal destruction of the graphitic network of the carbons nanodiscs. In the case of oxCNDs a continuous weight loss is observed at the temperature range between 140 and 320 ^oC; we attribute this loss to the removal of the oxygen containing groups (hydroxyl, carboxyl, epoxy) covalently attached to the graphitic layers of CNDs. The drop in the mass is estimated to be 25 wt% indicating the degree

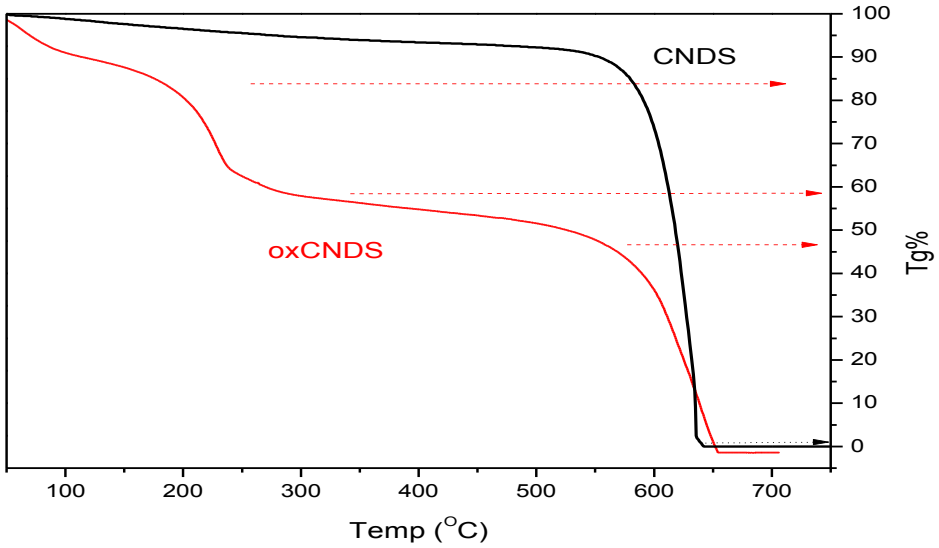

Figure 4.4. Weight loss curves collected during the thermogravimetric analysis of pristine (black) and oxidized carbon nanodiscs (red).

of functionalization that has occurred upon oxidation of the pristine CNDs. Moreover, carbon combustion (decomposition of graphitic lattice) occurs at lower temperatures compared to pristine CNDs, namely around 440 ^{o}C, since the presence of oxygenated species facilitates an accelerated graphitic network combustion.

The X-ray diffraction patterns of pristine and oxidized carbon nanodiscs are presented in Figure 4.5a. Pristine CNDs display a well-defined peak at 26.6^{o}, which is attributed to the 002 reflection of the graphite lattice and mirrors a basal spacing d_{002}=3.4 Å. In the case of oxCNDs this diffraction peak disappears and a new sharp one is present at lower angles (~11.4 ^{o}). The latter is due to the principal 001 reflection and corresponds to a basal spacing of d_{001}= 7.7 Å, indicative of the successful oxidation of graphitic layers of the CNDs with the creation of oxygen-containing groups that are randomly distributed on the basal planes and edges of the graphenic nanodiscs.

The morphology of the oxidized nanodiscs was examined thoroughly with AFM microscopy. Figure 4.5b shows a representative micrograph of isolated nanodiscs

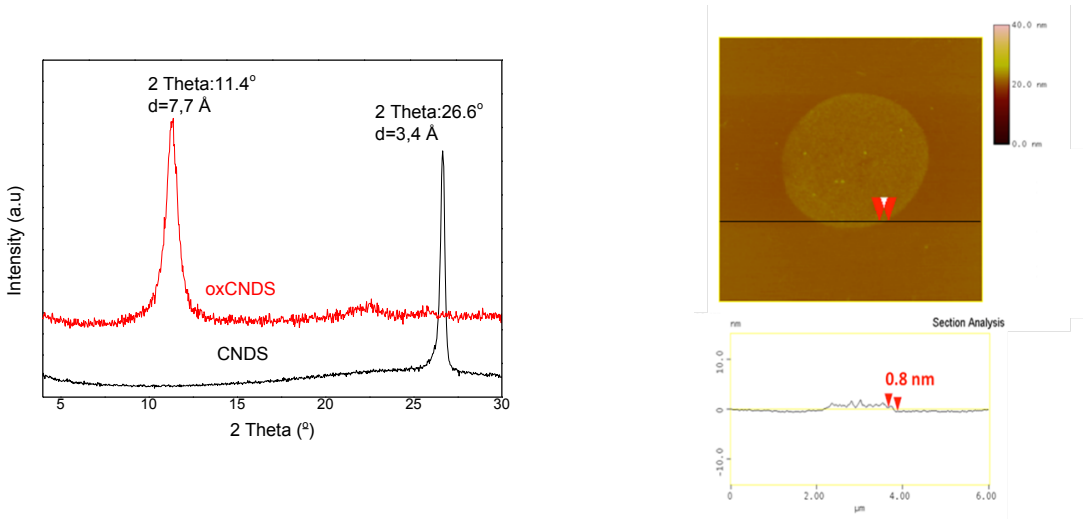

Figure 4. 5. X-ray diffraction patterns (a) pristine (black|) and oxidized carbon nanodisks (red), (b) AFM image of oxCNDs.

with a thickness of 0.8 Å, as calculated from topographical height profile These monoatomic graphitic nanodiscs are the majority of the scanned area. However, nanodiscs with thickness between 2 and 5 nm are also present, indicating the occurrence of larger discs consisted of several graphitic layers.

In view of possible applications for these new oxidized nanocarbons we tested whether oxCNDs can be used as cytotoxic agent on human embryonic kidney Hek293T and human adenocarcinoma HeLa cell lines. The results of the cell viability assays shown in Figures 4.6 and 4.7. Figure 4.6 shows the absorbance related to mitochondrial redox function, indicative of cell viability of the cell lines. When oxCNDs in the range of 0 μg/ml- 1mg/ml are added, we can observe that comparing the effect of oxCNDs on both Hek293T (healthy) and HeLa (cancer) cells, HeLa cells are effected more by the presence of oxCNDs. A way to quantify this effect is to determine the half maximal inhibitory concentration or IC_{50} values for both cell lines, *i.e.* the concentration oxCNDs required for 50 % inhibition of cell growth. As we see in Figure 4.7, in the case of Hek293T cell line IC_{50} amounts to 82 μg/ml. In other words,

for this concentration half of the cells (50%) are still alive after adding the oxCNDs. On the other hand, in the case of HeLa cancer cells, only 33 µg/ml are needed to achieve the same effect. Therefore oxCNDs are a very promising hybrid material suitable not only as an effective support for enzyme immobilization for the development of nanobiocatalytic systems as reported previously[40]but also antiproliferative agent on a specific cancer line.

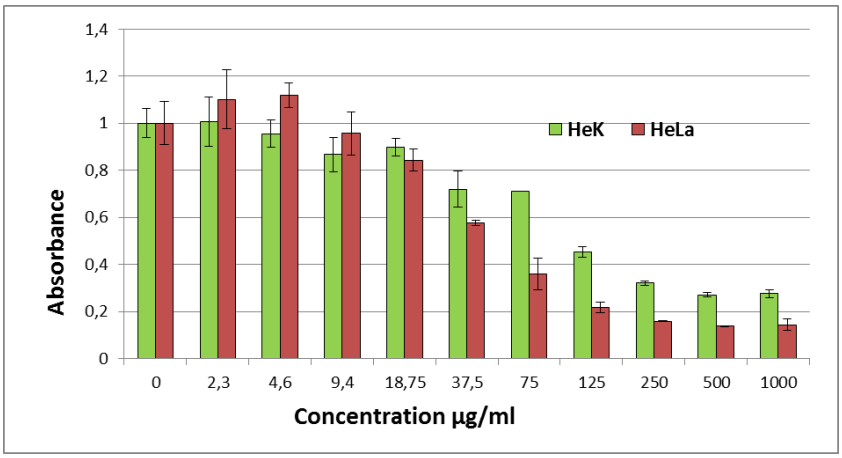

Figure 4.6. Absorbance % graph of oxCNDs for Hek293T (green) and HeLa(red) cell lines for concentration 0 µg-1000 µg.

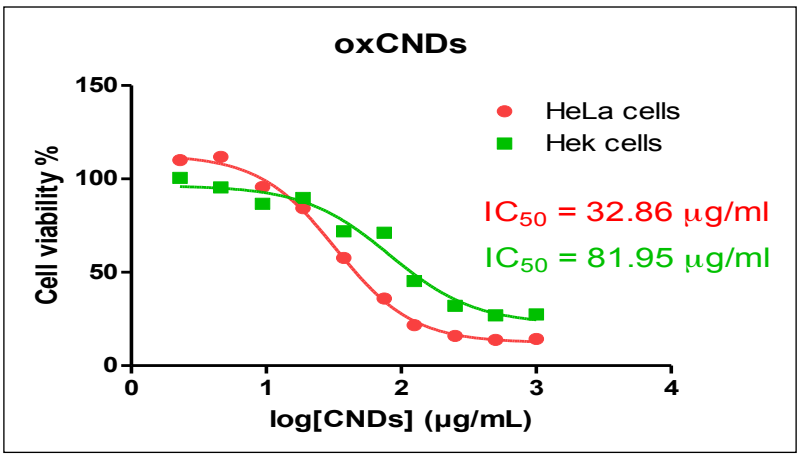

Figure 4.7. IC_{50} graph of oxCNDs for Hek293T (green) and HeLa (red) cell lines.

4.3. Conclusions

Insoluble carbon nanodiscs produced by the CB&H_2 process were successfully oxidized using a simple approach based on the well-known Staudenmaier's method. After strong acid treatment the surface of the CNDs is decorated with various oxygen-containing functional polar groups such as hydroxyl, carboxyl and epoxy groups, converting the completely insoluble CNDs into a hydrophilic derivative that is dispersible in many polar solvents, including water. X-ray diffraction, FTIR, XPS and Raman spectroscopies confirm the successful chemical functionalization and the presence of oxygen-containing functional groups covalently attached on the oxCNDs. Thermogravimetric and differential thermal analysis showed the high degree of functionalization of the pristine CNDs. Morphology studies by AFM microscopy show that the material is composed mainly of isolated monoatomic graphenic nanodiscs with a mean diameter in the range of 1 and 2 μm and a thickness of 0.8 Å; a small minority of few layer flakes is also observed. These hydrophilic nanostructures were tested as cytotoxic agents. Cell viability assays revealed that oxCNDs exhibited significant higher cytoxic activity on adenocarcinoma HeLa cell lines than on human embryonic kidney Hek293T cells, indicating that oxidized carbon nanodiscs is a very promising hybrid material for future biomedical applications.

References

[1] J. Ginsberg, *American Chemical Society* **2010**, **(*Commemorati*ve Booklet).**

[2] A. K. Geim, K. S. Novoselov, *Nat Mater* **2007**, *6*, 183–191.

[3] J. Wu, W. Pisula, K. Müllen, *Chemical Reviews* **2007**, *107*, 718–747.

[4] F. Wang, D. Kozawa, Y. Miyauchi, K. Hiraoka, S. Mouri, Y. Ohno, K. Matsuda, *Nat Commun* **2015**, *6* **(*Article number: 6305,open access).***

[5] M. Patila, I. V Pavlidis, E. K. Diamanti, P. Katapodis, D. Gournis, H. Stamatis, *Process Biochemistry* **2013**, *48*, 1010–1017.

[6] A. Galano, *Nanoscale* **2010**, *2*, 373–380.

[7] P. Serp, M. Corrias, P. Kalck, *Applied Catalysis A: General* **2003**, *253*, 337–358.

[8] M. Inagaki, L. R. Radovic, *Carbon* **2002**, *40*, 2279–2282.

[9] S. Subramoney, *Advanced Materials* **1998**, *10*, 1157–1171.

[10] V. Georgakilas, D. Gournis, V. Tzitzios, L. Pasquato, D. M. Guldi, M. Prato, *Journal of Materials Chemistry* **2007**, *17*, 2679–2694.

[11] D. Tasis, N. Tagmatarchis, A. Bianco, M. Prato, *Chemical Reviews* **2006**, *106*, 1105–1136.

[12] R. Andrews, D. Jacques, D. Qian, T. Rantell, *Accounts of Chemical Research* **2002**, *35*, 1008–1017.

[13] H. He, C. Gao, *Chemistry of Materials* **2010**, *22*, 5054–5064.

[14] M. Moniruzzaman, K. I. Winey, *Macromolecules* **2006**, *39*, 5194–5205.

[15] P. K. Ang, S. Wang, Q. Bao, J. T. L. Thong, K. P. Loh, *ACS Nano* **2009**, *3*, 3587–3594.

[16] E. Frackowiak, F. Béguin, *Carbon* **2001**, *39*, 937–950.

[17] A. Kumar, A. L. M. Reddy, A. Mukherjee, M. Dubey, X. Zhan, N. Singh, L. Ci, W. E. Billups, J. Nagurny, G. Mital, et al., *ACS Nano* **2011**, *5*, 4345–4349.

[18] S. Lynum, J. Hugdahl, K. Hox, R. Hildrum, M. Nordvik, **2008 (patent)**.

[19] A. Krishnan, E. Dujardin, M. M. J. Treacy, J. Hugdahl, S. Lynum, T. W. Ebbesen, *Nature* **1997**, *388*, 451–454.

[20] T. Garberg, S. N. Naess, G. Helgesen, K. D. Knudsen, G. Kopstad, A. Elgsaeter, *Carbon* **2008**, *46*, 1535–1543.

[21] W. Zhang, M. Dubois, K. Guérin, P. Bonnet, E. Petit, N. Delpuech, D. Albertini, F. Masin, A. Hamwi, *Carbon* **2009**, *47*, 2763–2775.

[22] H. L. Poh, F. Sanek, A. Ambrosi, G. Zhao, Z. Sofer, M. Pumera, *Nanoscale* **2012**, *4*, 3515–3522.

[23] R. Y. N. Gengler, A. Veligura, A. Enotiadis, E. K. Diamanti, D. Gournis, C. Józsa, B. J. van Wees, P. Rudolf, *Small* **2010**, *6*, 35–39.

[24] D. V Stergiou, E. K. Diamanti, D. Gournis, M. I. Prodromidis, *Electrochemistry Communications* **2010**, *12*, 1307–1309.

[25] D. W. Lee, L. De Los Santos V., J. W. Seo, L. L. Felix, A. Bustamante D., J. M. Cole, C. H. W. Barnes, *The Journal of Physical Chemistry B* **2010**, *114*, 5723–5728.

[26] K. Spyrou, G. Potsi, E. K. Diamanti, X. Ke, E. Serestatidou, I. I. Verginadis, A. P. Velalopoulou, A. M. Evangelou, Y. Deligiannakis, G. Van Tendeloo, et al., *Advanced Functional Materials* **2014**, *24*, 5841–5850.

[27] D. Yang, A. Velamakanni, G. Bozoklu, S. Park, M. Stoller, R. D. Piner, S. Stankovich, I. Jung, D. A. Field, C. A. Ventrice Jr., et al., *Carbon* **2009**, *47*, 145–152.

[28] T. Tsoufis, F. Katsaros, Z. Sideratou, G. Romanos, O. Ivashenko, P. Rudolf, B. J. Kooi, S. Papageorgiou, M. A. Karakassides, *Chemical Communications* **2014**, *50*,

10967–10970.

[29] J. W. Chiou, S. C. Ray, S. I. Peng, C. H. Chuang, B. Y. Wang, H. M. Tsai, C. W. Pao, H.-J. Lin, Y. C. Shao, Y. F. Wang, et al., *The Journal of Physical Chemistry C* **2012**, *116*, 16251–16258.

[30] N. Mahato, N. Parveen, M. H. Cho, *Materials Express* **.**, *5*, 471–479.

[31] M. Acik, C. Mattevi, C. Gong, G. Lee, K. Cho, M. Chhowalla, Y. J. Chabal, *ACS Nano* **2010**, *4*, 5861–5868.

[32] D. Long, W. Li, L. Ling, J. Miyawaki, I. Mochida, S.-H. Yoon, *Langmuir* **2010**, *26*, 16096–16102.

[33] D. C. Marcano, D. V Kosynkin, J. M. Berlin, A. Sinitskii, Z. Sun, A. Slesarev, L. B. Alemany, W. Lu, J. M. Tour, *ACS Nano* **2010**, *4*, 4806–4814.

[34] C. Mattevi, G. Eda, S. Agnoli, S. Miller, K. A. Mkhoyan, O. Celik, D. Mastrogiovanni, G. Granozzi, E. Garfunkel, M. Chhowalla, *Advanced Functional Materials* **2009**, *19*, 2577–2583.

[35] A. C. Ferrari, J. C. Meyer, V. Scardaci, C. Casiraghi, M. Lazzeri, F. Mauri, S. Piscanec, D. Jiang, K. S. Novoselov, S. Roth, et al., *Physical Review Letters* **2006**, *97*, 187401.

[36] F. Torrisi, T. Hasan, W. Wu, Z. Sun, A. Lombardo, T. S. Kulmala, G.-W. Hsieh, S. Jung, F. Bonaccorso, P. J. Paul, et al., *ACS Nano* **2012**, *6*, 2992–3006.

[37] R. Saito, A. Jorio, A. G. Souza Filho, G. Dresselhaus, M. S. Dresselhaus, M. A. Pimenta, *Physical Review Letters* **2001**, *88*, 27401.

[38] C. Thomsen, S. Reich, *Physical Review Letters* **2000**, *85*, 5214–5217.

[39] F. Tuinstra, *The Journal of Chemical Physics* **1970**, *53*, 1126.

[40] P. Zygouri, T. Tsoufis, A. Kouloumpis, M. Patila, G. Potsi, Z. Sideratou, H.

Katsaros, Fotios Charalambopoulou, Georgia, Stamatis, P. Rudolf, T. A. Steriotis, D. Gournis, *To be submitted* **.**